

Inhibition of mild steel corrosion in HCl solution using chitosan

Saviour A. Umoren · Mauro J. Banera ·
Teodoro Alonso-Garcia · Claudio A. Gervasi ·
Maria V. Mirífico

Received: 10 May 2013 / Accepted: 4 August 2013 / Published online: 15 August 2013
© Springer Science+Business Media Dordrecht 2013

Abstract The efficiency of chitosan (a naturally occurring polymer) as a corrosion inhibitor for mild steel in 0.1 M HCl was investigated by gravimetric, potentiodynamic polarization, electrochemical impedance spectroscopy measurements, scanning electron microscopy, and UV–visible analysis. The polymer was found to inhibit corrosion even at a very low concentration. Inhibition efficiency increases with a rise in temperature up to 96 % at 60 °C and then drops to 93 % at 70 °C, while it slightly increases with an increase in

chitosan concentration. Polarization curves indicate that chitosan functions as a mixed inhibitor, affecting both cathodic and anodic partial reactions. Impedance results indicate that chitosan was adsorbed on the metal/solution interface. Adsorption of chitosan at the mild steel surface is found to be in agreement with Langmuir adsorption isotherm model. Chemical adsorption is the proposed mechanism for corrosion inhibition considering the trend of protection efficiency with temperature. Calculated kinetic and thermodynamic parameters corroborate the proposed mechanism.

Keywords Chitosan · Mild steel · Acid corrosion · Corrosion inhibition · Natural polymer

S. A. Umoren · M. J. Banera · C. A. Gervasi ·
M. V. Mirífico (✉)
Departamento de Química, Facultad de Ciencias Exactas,
Instituto de Investigaciones Fisicoquímicas Teóricas y
Aplicadas (INIFTA, CCT La Plata-CONICET),
Universidad Nacional de La Plata, Casilla de Correo 16,
Sucursal 4, 1900 La Plata, Argentina
e-mail: mirifi@inifta.unlp.edu.ar

S. A. Umoren
Department of Chemistry, Faculty of Science,
University of Uyo, Uyo, Nigeria
e-mail: saviourumoren@yahoo.com

T. Alonso-Garcia
Biosurfaces Unit, CIC biomaGUNE, Paseo Miramón
182 C, 20009 San Sebastián, Gipuzkoa, Spain

C. A. Gervasi · M. V. Mirífico
Laboratorio de Ingeniería de Corrosión y Tecnología
Electroquímica (LICTE), Facultad de Ingeniería, UNLP,
1 y 47, 1900 La Plata, Argentina

Introduction

Mineral acids (in particular HCl) are widely used to remove iron oxide/rust in several industrial processes such as acid pickling, acid cleaning, acid descaling and oil well acidizing (Ahmad et al. 2010; Nataraja et al. 2011). Acids enhance the rate of metal dissolution and are indirectly responsible for the failure of the material. A useful method to protect metals and alloys deployed in service in such aggressive environments against corrosion is the addition of species to the solution in contact with the metallic surface in order to inhibit the corrosion reaction and reduce the corro-

sion rate. The use of organic compounds to inhibit corrosion of mild steel in acid environments is well established [Singh 2012; Machnikova et al. 2008; Fu et al. 2012; Obi-Egbedi and Obot 2011; Behpour et al. 2009a, b).

Unfortunately, most of the organic inhibitors are toxic, very expensive, environmentally unfriendly and non biodegradable. Due to increasing environmental awareness and adverse effect of some chemicals, research activities in recent times are geared towards developing cheap, non-toxic and environmentally acceptable and biodegradable corrosion inhibitors.

Naturally occurring polymers can readily satisfy these requirements and some of them have been shown to function as effective inhibitors of metal corrosion in different aggressive environments. For instance Solomon et al. (2010), Bayol et al. (2008) and Khairou and El-sayed (2003) have reported carboxymethyl cellulose (CMC) as effective corrosion inhibitor for mild steel in H_2SO_4 , mild steel and cadmium in HCl solutions, respectively. Gum Arabic has been reported to inhibit the corrosion of mild steel and aluminium in H_2SO_4 solution (Umoren 2008) and aluminium in NaOH solution (Umoren et al. 2006). Abdallah (2004) investigated the corrosion inhibition of carbon steel in H_2SO_4 using guar gum. Results obtained showed that guar gum acts as an inhibitor for acid-induced corrosion of carbon steel and an inhibition efficiency value of 93.88 % was obtained for a concentration of 1,500 ppm. The use of tapioca starch to improve the corrosion resistance of aluminium alloy AA6061 in sea water has been reported by Rosliza and Wan Nik (2010) and for mild steel corrosion inhibition in H_2SO_4 solution (Mobin et al. 2011) as well. The inhibitive effect of the gum exudate from *Acacia seyal* var. *seyal* on the corrosion of mild steel in drinking water has also been reported by Buchweishaija and Mhinzi (2008). Likewise, exudates gums from *Raphia hookeri* and *Pachlobus edulis* for inhibition of mild steel and aluminium corrosion in acidic medium have been reported (Umoren et al. 2008, 2009).

Chitosan, the subject of the present investigation is the fully or partially deacetylated product of chitin, the second most abundant natural resource next to cellulose. Because chitosan is biocompatible, biodegradable and almost nontoxic material, it has been used widely in the pharmaceutical field as a carrier for drug delivery and as a biomedical material (Yang et al. 2007). Moreover, chitosan shows some biological

activities such as immunological, antibacterial and wound healing activities and has been proposed for tissue engineering applications (Yang et al. 2007). In addition to its applications in medicine, chitosan is used in cosmetics, textile, paper, food and many other industrial branches (Jayakumar et al. 2005).

Examination of the molecular structure of chitosan shown in Fig. 1 reveals the presence of amino and hydroxyl groups which offer the possibility of ionic interactions with a metal surface, hence fulfilling an important criterion to function as a corrosion inhibitor. It has been reported as efficient green corrosion inhibitor with efficiency of up to 95 % for copper in 0.5 M HCl (El-Haddad 2013). However, there has been no report, to the best of our knowledge, on the corrosion inhibition effect of chitosan for mild steel in acidic medium although there are some reports for its derivatives. For example, acetyl thiourea chitosan has been reported as effective corrosion inhibitor for mild steel in 0.5 M H_2SO_4 solution (Fekry and Mohamed 2010). Cheng et al. (2007) has also reported on carboxymethyl chitosan (a naturally occurring polymer) as an ecofriendly inhibitor for mild steel in HCl solution. The ability of chitosan-crotonaldehyde Schiff's base to inhibit mild steel corrosion in aerated 3 % NaCl solution has been reported by Mohamed and Fekry (2011).

The present work was undertaken to assess the corrosion inhibition capability of unmodified chitosan

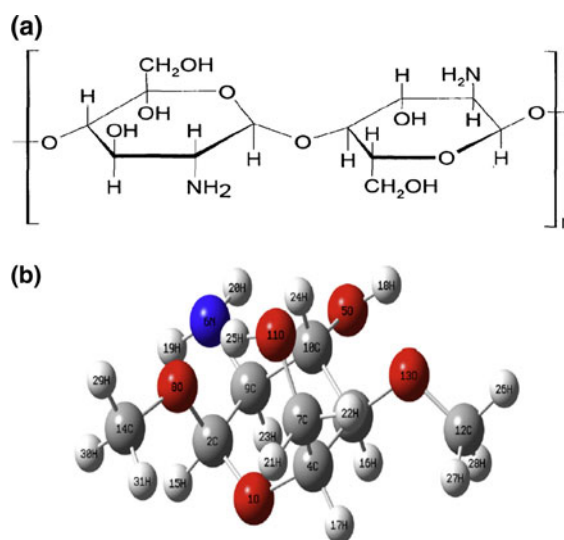


Fig. 1 **a** Chemical structure of chitosan and **b** optimized chemical structure

for mild steel in HCl solution using the weight loss method together with electrochemical techniques, in the 30–70 °C temperature range, while morphological changes of the corroding steel surface in the absence and presence of chitosan were observed by scanning electron microscopy (SEM).

Experimental

Materials preparation

Corrosion experiments were performed on mild steel specimens with weight percentage composition as follows: C-0.21; Mn-0.9; P-0.022; Si-0.03; S-0.030; Cr-0.11; Ni-0.12; Mo-0.022; Al-0.07; Cu-0.15 and the balance Fe. The corrosive medium was 0.1 M HCl (Merck) prepared from 37 % analytical grade reagent. Chitosan (Acros Organics, USA) with number average molecular weight, M_n , 200,000 g mol⁻¹ was used as the test inhibitor in the concentration range 0.4–4.0 μM. Firstly, a stock solution (4.0 μM) of chitosan was prepared by dissolving chitosan (0.8000 g) in 0.1 M HCl (1 L) in the presence of 0.3 M acetic acid (20 mL) to aid complete dissolution (Rinaudo et al. 1999). Other concentrations for the test solutions were obtained by serial dilution of the stock solution.

Weight loss measurements

Weight loss experiments were conducted on test coupons of dimension 3 cm × 3 cm × 0.14 cm. These coupons were wet-ground with silicon carbide abrasive paper (from grade #400 to #1200), rinsed with distilled water, degreased with acetone and dried with warm air, weighed, and stored in moisture-free desiccators prior to use. Triplicate samples of the cleaned weighed coupons were freely suspended in glass reaction vessels containing the test solutions. Experiments were conducted under total immersion conditions in 250 mL of the naturally aerated and unstirred test solutions that were kept within the (30–70) ± 1 °C temperature range using a thermostated water bath. To determine weight loss, the coupons were retrieved after 5 h of immersion, placed in 20 % NaOH solution containing 200 g/L of zinc dust, scrubbed with a bristle brush, washed with copious water and then with acetone, dried, and weighed. The difference between the weight of the

coupons after 5 h of immersion and its initial weight was taken to be the weight loss. Data for triplicate determinations showed good reproducibility which was greater than 95 %. From weight loss values, corrosion rates (C_R) were computed using the following expression:

$$C_R = \frac{m_1 - m_2}{At} \quad (1)$$

where m_1 and m_2 are weights (g) of mild steel coupons before and after immersion, respectively, in test solutions, A is the exposed area of a specimen (cm²) and t is the immersion time (h).

The inhibition efficiency ($\eta\%$) of chitosan was evaluated from the following equation:

$$\eta\% = \frac{C_{R(blank)} - C_{R(inh)}}{C_{R(blank)}} \times 100 \quad (2)$$

where $C_{R(blank)}$ and $C_{R(inh)}$ are the corrosion rates in 0.1 M HCl in the absence and presence of the inhibitor, respectively, at the same temperature.

Weight loss, CR and $\eta\%$ data presented here correspond to average values.

Electrochemical measurements

Test metal samples for electrochemical experiments were machined into cylindrical specimens and then embedded in polytetrafluoroethylene (PTFE) with an exposed geometrical circular area of 0.283 cm². The exposed surface was also cleaned as described above. Electrochemical experiments were conducted in a three-electrode electrochemical cell using a PAR potentiostat model 273A controlled by a personal computer for polarization studies and a Zahner IM6 electrochemical workstation for electrochemical impedance spectroscopy (EIS) studies. A platinum sheet was used as the counter electrode, and a saturated calomel electrode (SCE) was used as the reference electrode. The latter was connected via a Luggin's capillary. All potentials in this work are referred to the SCE (0.2412 V with respect to the standard hydrogen electrode). Measurements were performed in naturally aerated and unstirred solutions at the end of 1 h of immersion at 30 ± 1 °C maintained using a thermostated water bath. Impedance measurements were made at the corrosion potential (E_{corr}) over a frequency range from 50 kHz to 5 mHz, with a perturbation signal amplitude of 10 mV. Potentiodynamic

polarization studies were carried out in the potential range \pm ca. 250 mV versus the corrosion potential at a scan rate of 0.333 mVs^{-1} . Each test was run in triplicate to verify the reproducibility of the data.

UV–visible spectrophotometric measurements

UV–visible absorption spectrophotometric measurements were carried out for 0.1 M HCl solution without and with $4.0 \mu\text{M}$ chitosan before and after mild steel samples immersion at $70 \pm 1 \text{ }^\circ\text{C}$ for 5 h. All spectra were recorded using a Shimadzu UV–1800 spectrophotometer.

SEM surface analysis

Morphological studies of the mild steel samples were undertaken by SEM examinations of surfaces exposed to different test solutions, using a Quanta 200 (FEI, Holland) scanning electron microscope operating with tungsten filament as electron source. Mild steel specimens of dimensions $3 \text{ cm} \times 3 \text{ cm} \times 0.14 \text{ cm}$ were ground successively with silicon carbide abrasive paper of different grades (#400–#1200) and thereafter polished using a cloth with $5 \mu\text{m}$ diamond paste to obtain a near mirror-like finish of the surface. The cleaned coupons were immersed for 5 h in the blank solution 0.1 HCl without and with $4.0 \mu\text{M}$ chitosan at $(40 \pm 1) \text{ }^\circ\text{C}$, and then washed with distilled water, dried in warm air, and submitted for SEM surface examination.

Results and discussion

Weight loss, corrosion rates and inhibition efficiency

The weight loss method uses a direct parameter for the quantitative evaluation of corrosion, that is, the loss in mass of the metal exposed to a corrosive medium over a specified period of time. The experimental results obtained for the corrosion behaviour of mild steel in 0.1 M HCl solution without and with different concentrations of chitosan (C) from the weight loss measurements are presented in Figs. 2 and 3. Figure 2a, b show plots of weight loss and corrosion rate (Eq. 1) as a function of inhibitor concentration at

different temperatures, respectively. The plots indicate that weight loss and consequently, the corrosion rate were reduced on addition of chitosan into the corrosive medium in comparison to the blank solution. This indicates that chitosan functioned as an inhibitor isolating the metal surface from the attack by the corrosive solution. Further inspection of the figures revealed that weight loss and corrosion rate of mild steel in the absence and presence of inhibitor increases with an increase in temperature. Also the decrease in weight loss and corrosion rate of the metal coupons on addition of chitosan was concentration dependent, namely, weight loss and corrosion rate decrease markedly as the concentration of chitosan increases up to $0.4 \mu\text{M}$, beyond this concentration the decrease becomes less noticeable.

The decrease in corrosion rate in the presence of chitosan results in a corresponding increase in inhibition efficiency (Eq. 2). Figure 3 shows the plot of inhibition efficiency against chitosan concentration at different temperatures. Examination of the plot revealed that inhibition efficiency increases marginally with increase in concentration of chitosan. This implies that chitosan acts as an effective inhibitor even at low concentration. Also inhibition efficiency is

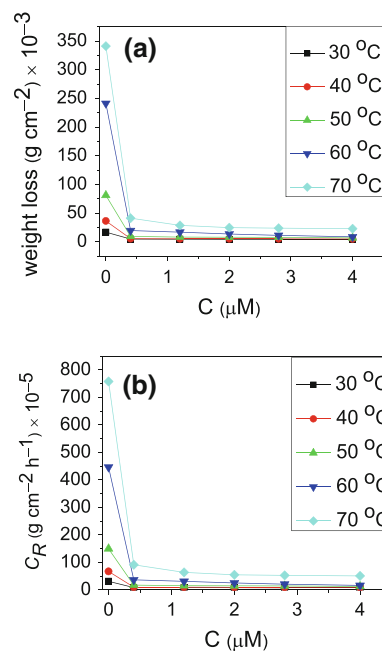


Fig. 2 Plot of **a** weight loss and **b** corrosion rate C_R against inhibitor concentration C, after 5 h of immersion, at different temperatures

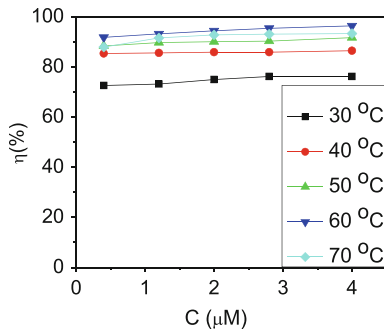


Fig. 3 Plot of inhibition efficiency $\eta(\%)$ against inhibitor concentration C at different temperatures

observed to increase with increase in temperature (T) (Fig. 4) up to a maximum value of 96 % at 60 °C which decreases to 93 % at 70 °C at the highest concentration of chitosan (4.0 μM) studied. The decrease in inhibition efficiency at higher temperature suggests a possible shift of the adsorption–desorption equilibrium towards desorption of the adsorbed inhibitor. In addition, the boost in solution agitation resulting from higher rates of hydrogen gas evolution as well as roughening of the metal surface as a result of enhanced corrosion may also reduce the ability of the inhibitor to become adsorbed on the metal surface at elevated temperatures (Oguzie 2006). Corrosion inhibition is thought to be initiated by the displacement of adsorbed water molecules by the inhibitor species leading to the specific adsorption of the inhibitor on the metal surface (Umoren 2011). Examinations of the chemical structure of chitosan repeat units (Fig. 1) reveal that it contains O and N heteroatoms. The adsorption of chitosan through these heteroatoms onto the mild steel surface will create a barrier for charge and mass transfers and thus isolate the metal from further attack from the corrosive agents present in solution, hence the observed inhibiting effect.

Potentiodynamic polarization measurements

Kinetics of the anodic and cathodic reactions occurring on mild steel electrodes in 0.1 M HCl solutions in the absence and presence of different concentrations of chitosan was investigated using potentiodynamic polarization measurements. Figure 5 shows typical potentiodynamic polarization curves for the mild steel sample in 0.1 M HCl without and with different concentrations of chitosan. From Fig. 5, the mild steel

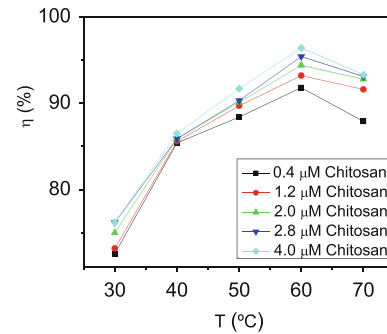


Fig. 4 Plot of inhibition efficiency $\eta(\%)$ against temperature T at different inhibitor concentrations

specimen is seen to exhibit active dissolution with no distinctive transition to passivation within the studied potential range in all environments, as expected for highly acidic solutions. Further examination of the plots in Fig. 5 reveals only negligible shifts in E_{corr} . The small changes in E_{corr} may be the result of the competition of the anodic and the cathodic inhibited reactions, and of the metal surface condition (Stupnisek-Lisac et al. 2002). A decrease in both cathodic and anodic currents is observed. This result indicates how the addition of chitosan hindered attack on the mild steel electrode by the acid aggressive solution.

Values of corrosion current density (i_{corr}), corrosion potential (E_{corr}), polarization resistance (R_p) and inhibition efficiency ($\eta\%$) calculated from polarization data are presented in Table 1. Polarization resistance values were determined directly from the low-overvoltage (non-Tafel) region through curve-fitting procedures (Jones 1992; Mansfeld 1973).

Polarization resistances, R_p for mild steel in 0.1 M HCl solution, in the absence and in the presence of different concentrations of added chitosan, were determined from the current–potential curves in the

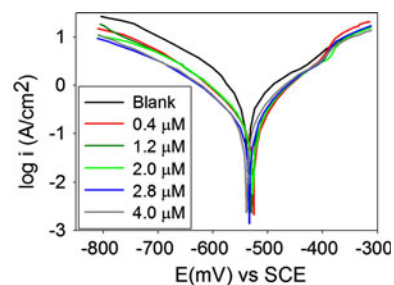


Fig. 5 Potentiodynamic polarization curves for mild steel in 0.1 M HCl in the absence and presence of different concentrations of chitosan, after 1 h of immersion, at 30 ± 1 °C

Table 1 Parameters obtained from potentiodynamic polarization curves for mild steel in 0.1 M HCl solution in the absence and presence of chitosan (see text for the parameters definitions), after 1 h of immersion at 30 ± 1 °C

Chitosan concentration (μM)	E_{corr} (mV/SCE)	i_{corr} ($\mu\text{A cm}^{-2}$)	R_p ($\Omega \text{ cm}^2$)	η
Blank	−540	594	40	–
0.4	−529	205	117	65.5
1.2	−530	199	108	66.5
2.0	−530	214	102	63.9
2.8	−535	185	127	68.9
4.0	−538	190	120	68.0

vicinity of E_{corr} . Straight lines were obtained in the potential range $E_{\text{corr}} \pm 20$ mV from which the values listed in Table 1 were obtained. The decrease in the rate of corrosion (i_{corr}) after the introduction of chitosan into the corrosive medium is associated with the shift of both cathodic and anodic Tafel branches of the polarization curves towards lower current density values. This behaviour indicates inhibition of both the hydrogen evolution and mild steel dissolution reactions. Therefore, chitosan can be classified as a mixed-type inhibitor. The polarization resistance is observed to increase in the presence of chitosan compared to the blank solution. Also, there is no appreciable increase in R_p values with an increase in inhibitor concentration, which is in agreement with the weight loss results. The inhibition efficiency ($\eta\%$) was computed using the equation:

$$\eta\% = \left(1 - \frac{i_{\text{corr}}}{i_{\text{corr}}^0}\right) \times 100 \quad (3)$$

where i_{corr}^0 and i_{corr} are the corrosion current densities in the absence and in the presence of the inhibitor, respectively. As noted with weight loss measurements, there is no appreciable change in the values of inhibition efficiency as chitosan concentration increased. However, $\eta\%$ values obtained from the polarization method are lower (ca. 30 %), something that could probably be attributed to insufficient time for the inhibitor to get adsorbed on the mild steel surface.

The modes of the inhibition effect of organic compounds are classified into three categories: geometric blocking effect of adsorbed inhibitive species, active sites blocking effect by adsorbed inhibitive

species, and electro-catalytic effect of the inhibitor or its reaction products (Okafor and Zheng 2009; Cao 1996; Behpour et al. 2009a, b). It has been claimed that in the case of the first mode the inhibition effect results from the reduction of the reaction area on the surface of the corroding metal, whereas for the other two modes the inhibition effects are due to changes in the average activation energy barriers of the anodic and cathodic reactions of the corrosion process.

Electrochemical impedance spectroscopy measurements

EIS experiments were undertaken mainly, as an independent and complementary tool to determine corrosion rates in a rapid and accurate way. EIS also allows gaining insight into the characteristics and kinetics of electrochemical processes which occur at mild steel/0.1 M HCl interface and how this is modified by the presence of chitosan. Figure 6 shows the impedance spectra as exemplified by Nyquist plots obtained for mild steel in the absence and presence of different concentrations of chitosan. Nyquist plots typically show a single depressed capacitive semicircle for the blank solution over the frequency range studied. However, in the presence of chitosan the Nyquist diagrams are characterized by a large capacitive loop at high to medium frequency and an inductive loop at low frequency. The capacitive loop at high frequencies contains double layer charging effects. Additionally, this capacitive loop reflects resistive phenomena due to the charge transfer resistance that is a part of the Faradaic impedance of the reaction interface (Abd El Rehim et al. 2001; Khaled and Al-Qahtani 2009). The presence of an inductive loop has been attributed to relaxation of adsorbed reaction intermediates on the electrode surface, exhibiting negative change in the surface coverage with potential on the surface of the metal (Bai and Conway 1991; Okafor and Zheng 2009). Inspection of Fig. 6 also reveals that addition of chitosan to the corrosive medium results in a marked increase in size of the semicircle in Nyquist plot compared to the blank solution, which is an indication of the inhibition of the corrosion process. However, only a slight increase in the size of the semicircle was observed with increase in the concentration of chitosan, which is in agreement with the results obtained with weight loss and polarization measurements. It can also be observed

that capacitive responses in the presence of chitosan correspond to depressed semicircles with the centre below the real axis. This kind of behaviour is typical of solid metal electrodes that show frequency dispersion (Khaled et al. 2006).

Spectra for the experimental impedance data were analyzed using an equivalent circuit model for the blank solution that using Boukamp’s notation the circuit description code reads Rs(Qo(R1(R2C1))) (not shown) (Boukamp 1986). R_p corresponds here to the sum ($R_1 + R_2$) according to Eq. (9) below. The complex impedance diagram for mild steel in 0.1 M HCl in the presence of chitosan is shown in Fig. 7a, while the equivalent circuit used to fit the experimental data is presented in Fig. 7b. It consists of constant phase element (CPE) Q in parallel with series resistors R_1 and R_2 , and an inductance, of magnitude L, in parallel connection with R_2 . Accordingly, the total impedance Z_{total} is equal to the sum of R_s and Z_1 , where Z_1 is

$$Z_1 = \left(\frac{1}{Z_{CPE}} + \frac{1}{Z_2 + R_1} \right)^{-1} \tag{4}$$

and Z_2 is

$$Z_2 = \left(\frac{1}{R_2} + \frac{1}{j\omega L} \right)^{-1} \tag{5}$$

$$Z_2 = \frac{R_2^2 L(j\omega) + R_2 L^2 \omega^2}{R_2^2 + \omega^2 L^2} \tag{6}$$

Hence, the total impedance is given by

$$Z_{total} = R_s + \left\{ Q(j\omega)^n \left(\frac{R_2^2 L(j\omega) + R_2 L^2 \omega^2}{R_2^2 + \omega^2 L^2} + R_1 \right) \right\}^{-1} \tag{7}$$

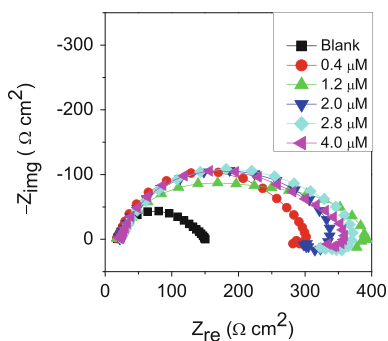


Fig. 6 Nyquist plots of mild steel in 0.1 M HCl in the absence and presence of chitosan

The use of a CPE-type impedance has been extensively described in the literature for this type of studies. Again, although a frequency elevated to a fractional exponent may be questionable from a physical point of view, for the interpretative objective explained above, the use of a CPE impedance element is useful in this work. Normally, exponent n in Eq. 8 for CPE impedance is understood in terms of the degree of non-ideality in capacitive behaviour that in this work is related to the electrical double layer.

$$Z_{CPE} = [Q(j\omega)^n]^{-1} \tag{8}$$

The exponent value makes it possible to differentiate the behaviour of a CPE ($n < 1$) from that of an ideal capacitor ($n = 1$). In the complex impedance plot Fig. 7a, the value of R_p corresponds to the intercept of the impedance diagram with the real axis for $\omega \rightarrow 0$:

$$R_p = \lim_{\omega \rightarrow 0} [Z_{real}] \tag{9}$$

where Z_{real} denotes the real part of the faradaic impedance which according to the considered equivalent circuit is equal to the sum $Z_2 + R_1$.

The polarization resistance, R_p is correlated unequivocally to the corrosion current density in

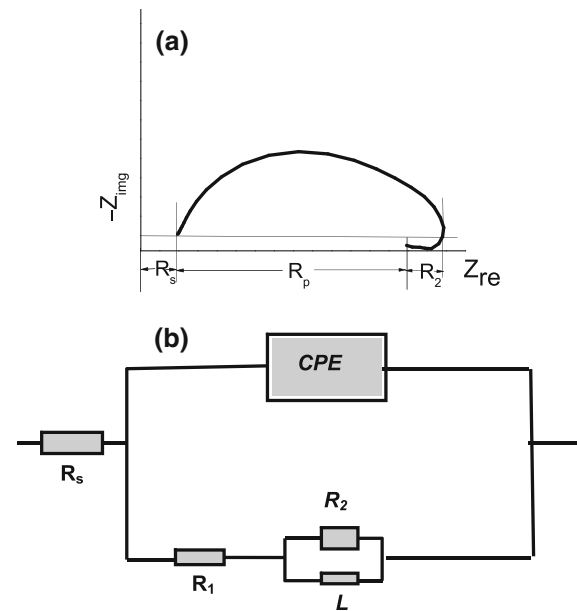


Fig. 7 Schematic representation of impedance data in the complex plane (a) and the equivalent circuit used to fit experimental data in the presence of chitosan (b)

relatively simple corrosion systems characterized only by a charge transfer-controlled process (Metikos-Hukovic et al. 2002). For each set of experimental data, the parameters Q_1 , R_1 , R_2 and L were evaluated using a procedure involving complex nonlinear least squares fitting. The experimental data were found to be sufficiently well fitted by the transfer function of the equivalent circuit presented in Fig. 7, within the limits of experimental error and reproducibility of the data (see Fig. 8). At this point it is perhaps worth remembering that the interpretation of an inductive loop has proved to be one of the most difficult problems in connection with the use of EIS for corroding systems. Moreover, analyzing such spectra on the basis of an inductance or negative capacitance and resistance values can only be performed to obtain accurate values of R_p as a fit parameter but not to derive mechanistic information of the corroding system (Mansfeld 1999).

Fit values of the impedance parameters are listed in Tables 2 and 3 for the blank solution and for solutions containing chitosan, respectively. Results in the tables show that the value of the polarization resistance increased in the presence of chitosan in comparison to the blank solution. Also it is observed that there is no appreciable change in the value of the polarization resistance with increase in concentration of chitosan. The inhibition efficiency was computed using the following equation (Noor 2009):

$$\eta\% = \left(1 - R_p^0/R_p\right) \times 100 \quad (10)$$

where R_p^0 and R_p are the polarization resistances in the absence and presence of inhibitor (chitosan),

respectively and the values are listed in Tables 2 and 3. As observed with weight loss and polarization methods, the inhibition efficiency obtained from EIS measurements did not change significantly with increase in concentration of chitosan. However, comparison of inhibition efficiencies using ac (EIS) and dc (potentiodynamic polarization) methods shows that the values obtained from dc method are somewhat (up to 10 %) higher than those obtained from the ac technique, although the magnitude was the same for both techniques. Some authors (Oguzie et al. 2007) have pointed out that the differences in values of inhibition efficiency sometimes observed between EIS and polarization techniques could be attributed to a predominant influence of the anodic dissolution process in determining the corrosion rate from polarization measurements.

Adsorption isotherm

It is generally assumed that corrosion occurs on the uncovered parts of the metal surface and the corrosion of the covered part is almost equal to zero. Accordingly, the surface coverage (θ) was estimated for the different concentrations of chitosan from the weight loss data as follows: $\theta = \eta\%/100$ (assuming a direct relationship between inhibition efficiency and degree of surface coverage). The surface coverage values obtained were fitted to various adsorption isotherm models while the resulting correlation coefficient (R^2) was a useful means of determining the best fit isotherm. By far, the best result was obtained with the Langmuir adsorption isotherm, given as:

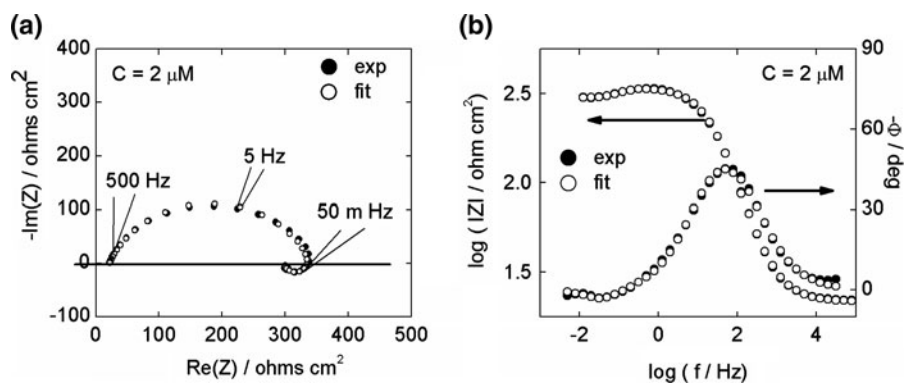


Fig. 8 Impedance spectra for a mild steel electrode in 0.1 M HCl containing 2.0 μM chitosan. Measured and fitted data represented as Nyquist diagrams (a) and Bode plots (b).

Experimental data (closed circle) and fit results (open circle) according to the equivalent circuit (Fig. 7)

Table 2 Electrochemical impedance parameters for mild steel in 0.1 M HCl blank solution, after 1 h of immersion, at 30 ± 1 °C

Chitosan concentration (μM)	R_s ($\Omega \text{ cm}^2$)	Y_o ($\Omega^{-1} \text{ s}^n \text{ cm}^{-2}$) $\times 10^{-4}$	n_o	C_1 (F cm^{-2}) $\times 10^{-2}$	R_p ($\Omega \text{ cm}^2$)
0 (blank)	18.6	26.1	0.82	1.9	129

Table 3 Electrochemical impedance parameters for mild steel in 0.1 M HCl solution in the presence of chitosan, after 1 h of immersion, at 30 ± 1 °C

Chitosan concentration (μM)	R_s ($\Omega \text{ cm}^2$)	Y_o ($\Omega \text{ s}^n \text{ cm}^{-2}$) $\times 10^{-4}$	n	L (H cm^2)	R_L ($\Omega \text{ cm}^2$)	R_p ($\Omega \text{ cm}^2$)	$\eta\%$
0.4	18.4	2.0	0.80	164	19.1	265	51.2
1.2	17.0	4.2	0.65	965	31.0	336	61.5
2.0	21.0	1.5	0.77	156	42.7	278	53.5
2.8	23.0	2.2	0.74	51	48.0	300	56.9
4.0	22.5	1.8	0.76	606	25.1	303	57.3

$$\frac{C}{\theta} = \frac{1}{K_{ads}} + C \quad (11)$$

where C is the concentration of the inhibitor and K_{ads} is the equilibrium constant of the adsorption–desorption process. The plot of C/θ against C is shown to be linear in Fig. 9. The slopes of the linear plots are 1.30, 1.15, 1.09, 1.03 and 1.06 at 30, 40, 50, 60 and 70 °C, respectively and R^2 at all temperatures being higher than 0.999. Langmuir isotherm is based on the assumption that all the adsorption sites are equivalent, that each site can accommodate only one molecule (monolayer adsorption), that the sorption enthalpy is independent of surface coverage and that the particle-binding occurs independently from the nearby sites being occupied or unoccupied, independent of surface coverage and under this condition, the slope should be unity. The values of the slopes at 50–70 °C indicate that the adsorption of chitosan on mild steel surface obeys well the isotherm. The significant departure of the slope from unity observed at 30 and 40 °C may be explained on the basis of the interaction among the adsorbed species on the surface of the metal. Given that chitosan is a large molecule with polar groups, it could be adsorbed on the cathodic and anodic sites of the metal surface and such adsorbed species may interact by mutual repulsion or attraction. It is therefore pertinent to say that the adsorption of chitosan on the steel surface at these temperatures can be more appropriately represented by the modified Langmuir equation suggested by Villamil et al. (1999) which takes into consideration the interactions between

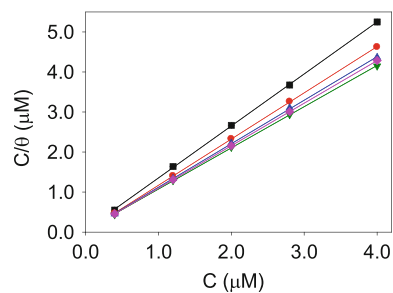
adsorbate species as well as changes in the heat of adsorption with changing surface coverage, as follows:

$$\frac{C}{\theta} = \frac{n}{K_{ads}} + nC \quad (12)$$

where n is the slope of the adsorption plot.

Adsorption parameters deduced from Langmuir adsorption isotherm (uncorrected) for mild steel corrosion in 0.1 M HCl obtained from weight loss measurements at different temperatures are listed in Table 4.

Negative values for ΔG_{ads}^o are universally considered in the literature as ensuring the spontaneity of the adsorption process and the stability of the adsorbed layer on the steel surface. To be precise, it is the value of ΔG rather than that of ΔG^o that serves as a criterion of spontaneous change under non-standard conditions at constant temperature and pressure. However, ΔG^o values are so readily available that this explains why

**Fig. 9** Langmuir adsorption isotherm for chitosan on mild steel in 0.1 M HCl at different temperatures (square 30 °C; circle 40 °C; inverted triangle 50 °C; diamond 60 °C; triangle 70 °C)

they are regularly used to get a rough idea of whether a given chemical change is possible.

Adsorption involves attracting molecules of chitosan to the metal surface. Thus, energy is released and adsorption is normally exothermic. Furthermore, physical adsorption involves weak forces of attraction and less heat evolves whereas chemical adsorption, involving strong forces of attraction, is related to a higher flow of heat released from the system. Physical adsorption is characterised by small enthalpy changes, rarely less than -25 kJ mol^{-1} , whereas chemisorption usually exhibits much more negative values below -40 kJ mol^{-1} (Atkins 1990). For the adsorption process ΔH is negative, while ΔS is also negative since chitosan molecules lose their translation freedom when they get attached to the surface of the adsorbent. Bearing in mind that $\Delta G = \Delta H - T\Delta S$ adsorption will spontaneously occur if $\Delta H > T\Delta S$.

Consequently, according to these widely accepted criteria the calculated values of $\Delta G_{\text{ads}}^{\circ}$ (Table 4), calculated from Eq. 13 and K_{ads} data in Table 4, represent an initial indication that the adsorption mechanism of chitosan on mild steel in 0.1 HCl solutions at the studied temperatures may be predominantly chemisorption.

$$K_{\text{ads}} = (1/55.5)\exp(-\Delta G_{\text{ads}}^{\circ}/RT) \quad (13)$$

As already indicated above, while the considered adsorption reaction carried out under standard conditions is characterized by a *single value* of $\Delta G_{\text{ads}}^{\circ}$, this process can have an infinite number of ΔG_{ads} values, reflecting the infinite possible compositions between the extremes of pure reactants and pure products. ΔG_{ads} values can be calculated according to the following relationship (Mortimer 2000).

$$\Delta G_{\text{ads}} = \Delta G_{\text{ads}}^{\circ} + RT \ln P \quad (14)$$

where P is the activity quotient.

Table 4 Adsorption parameters deduced from Langmuir adsorption isotherms for mild steel corrosion in 0.1 M HCl, at different temperatures

Temperature (°C)	$\Delta G_{\text{ads}}^{\circ}$ (kJ/mol)	K_{ads} (M^{-1}) $\times 10^{-6}$	Slope	R^2
30	-56.22	88.67	1.30	0.999
40	-57.49	71.67	1.15	0.999
50	-57.08	31.08	1.09	0.999
60	-58.12	23.80	1.03	0.999
70	-58.82	16.37	1.06	0.999

P can be calculated considering the following formal expression for the equimolar adsorption mechanism of chitosan (Chit) at vacant active surface-sites M to yield occupied surface-sites Chit(M) (monolayer adsorption according to the Langmuir mechanism (Ferreira et al. 2004).



Accordingly,

$$P = \theta/[(1 - \theta)C] \quad (16)$$

Thus, for a fixed global composition $P = 1$ results $\Delta G_{\text{ads}} = \Delta G_{\text{ads}}^{\circ}$ and $\theta = C/(1 + C)$. Since for the system under study, C is in the order of $10^{-6} \text{ M} \ll 1$ the coverage $\theta \cong C \cong 10^{-6}$ and as a result, this condition is met almost at the beginning of the reaction, with a composition of nearly pure reactants. Consequently, adsorption enthalpy and entropy changes can be derived from ΔG_{ads} ($P = 1$) values and correlated with the initial stages of the adsorption of chitosan. Plotting ΔG_{ads} ($P = 1$) versus T a straight line was obtained. From the corresponding ordinate and slope of this plot $\Delta H_{\text{ads}}(P = 1) = -42.7 \text{ kJ mol}^{-1}$ and $\Delta S_{\text{ads}}(P = 1) = -0.047 \text{ kJ K}^{-1} \text{ mol}^{-1}$ values were derived, respectively. These values indicate that the initial stage of adsorption evolves spontaneously towards the formation of occupied surface-sites, according to a route that results from a highly exothermic process with decreasing entropy, suggesting the occurrence of chemisorption, as discussed above.

Chemisorption was also interpreted as the major contributor to the adsorption mechanism judging from the increase of $\eta\%$ with increase in temperature and the lower values of the apparent activation energy for the corrosion process, E_a (see “Effect of temperature” section below), obtained in the presence of inhibitor as compared to its absence (Zarrouk et al. 2011). Comparable observations have been made regarding the adsorption of acetyl thiourea chitosan at 25 °C (Fekry and Mohamed 2010), carboxymethyl chitosan at 30 °C (Cheng et al. 2007) and pineapple leaf extract at 30 °C (Ekanem et al. 2010) on mild steel surface in HCl solution. It is perhaps worth repeating at this point that the experimentally measured inhibitory action of chitosan is not due to catalytic poisoning of the metal dissolution reaction but rather to an adsorption process that partially blocks the active area. In this sense, even though the presence of chitosan might kinetically enhance dissolution in the uncovered surface the final

result is a decrease in the magnitude of the net corrosion process.

Effect of temperature

The effect of temperature on the corrosion behaviour of mild steel in uninhibited and inhibited solutions containing different concentrations of chitosan was investigated in the 30–70 °C temperature range. The obtained results (Fig. 2a) show that rates of corrosion in absence and presence of the additive increased with a rise in temperature. This is a frequent behaviour since temperature elevation usually accelerates corrosive processes, particularly in media in which H₂ gas evolution accompanies corrosion (Noor 2007).

As already mentioned above, adsorption of an organic inhibitor can affect the corrosion rate by either decreasing the available reaction area (geometric blocking effect) or by modifying the activation energy of the anodic and/or cathodic reactions occurring in the inhibitor-free surface in the course of the inhibited corrosion process. The dependence of corrosion rate on temperature can be expressed by the Arrhenius equation:

$$\log C_R = \log A - \left(\frac{E_a}{2.303RT} \right) \quad (17)$$

where C_R is the corrosion rate, E_a is the apparent activation energy for the corrosion process, R is the molar gas constant, T is the absolute temperature, and A is the pre-exponential factor. Arrhenius plots, logarithm of corrosion rate ($\log C_R$) versus $1/T$, for mild steel in the corrodent (0.1 M HCl) without and with addition of different concentrations of chitosan are shown in Fig. 10. Straight lines were obtained with a slope of $(-E_a/2.303R)$ from which E_a values were computed and listed in Table 5. Analysis of the temperature dependence of inhibition efficiency as well as comparison of corrosion activation energies in absence and presence of the inhibitor gives some insight into the possible mechanism of inhibitor adsorption. A decrease in inhibition efficiency with a rise in temperature, with a corresponding increase in corrosion activation energy, in the presence of inhibitor (as compared to its absence), is frequently interpreted as an indication of physical adsorption, whereas the reverse effect, analogous to an increase in inhibition efficiency with rise in temperature and lower activation

energy in the presence of inhibitor, suggests a chemisorption mechanism (Martinez and Stern 2001; Popova et al. 2003).

Results in Table 5 show that E_a values are lower in the presence of the inhibitor than in its absence. This type of behaviour has been identified and discussed in detail by different authors (Amin et al. 2011). As explained above, this result does not contradict the measured inhibition of the corrosion process. Moreover, lower E_a values for the inhibited condition are in agreement with a lower anodic Tafel slope as measured in the presence of the chitosan and the formation of a complex species between Fe ions and chitosan molecules, as discussed below. The change of E_a according to the inhibitor concentration suggests chemical adsorption of chitosan on mild steel surface in the acidic environment and may be related to the modification of the metal dissolution mechanism. Temperature is a predominant factor in the formation of a protective layer at the metal/solution interface formed by metal-inhibitor interaction. This interaction between chitosan and the corroding mild steel specimen increases with temperature, resulting in enhanced surface coverage which decreases mild steel dissolution. Further inspection of Table 5 also revealed that E_a monotonously decreases with increasing chitosan concentration. The lowest E_a value (24.18 kJ mol⁻¹) was obtained at the highest chitosan concentration (4.0 μM) studied. Similar observations have been reported by Ekanem et al. (2010) and Noor (2007) in their studies of temperature effects on the corrosion inhibition of mild steel in acidic solutions by

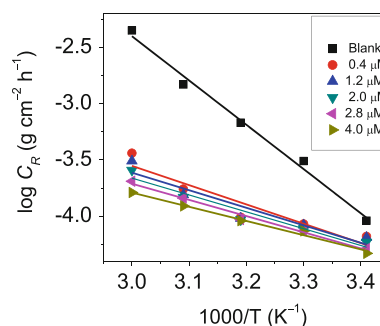


Fig. 10 Arrhenius plot for mild steel corrosion in 0.1 M HCl in the absence and presence of different concentrations of chitosan [square 0 μM (blank); circle 0.4 μM; triangle 1.2 μM; inverted triangle 2.0 μM; left slanting triangle: 2.8 μM; right slanting triangle 4.0 μM]

Table 5 Kinetic parameters for mild steel corrosion in 0.1 M HCl in the absence and presence of different concentrations of chitosan

Chitosan concentration (μM)	E_a (kJ mol^{-1})	ΔH^* (kJ mol^{-1})	ΔS^* ($\text{J mol}^{-1} \text{K}^{-1}$)
Blank	75.34	73.11	-72.4
0.4	32.79	30.00	-223.9
1.2	29.87	27.47	-232.6
2.0	28.69	25.55	-239.4
2.8	27.59	24.80	-242.5
4.0	24.18	21.39	-254.3

aqueous extract of pineapple leaves and Fenugreek, respectively.

The enthalpy of activation (ΔH^*) and the entropy of activation (ΔS^*) for the corrosion of mild steel in 0.1 M HCl without and with different concentrations of chitosan were obtained by applying transition state equation (Noor and Al-Moubaraki 2008):

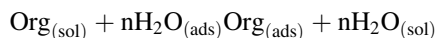
$$\log\left(\frac{C_R}{T}\right) = \left[\log\left(\frac{R}{Nh}\right) + \left(\frac{\Delta S^*}{2.303R}\right) \right] - \frac{\Delta H^*}{2.303RT} \quad (18)$$

where h is the Planck's constant, N is the Avogadro's number, and T is the absolute temperature. A plot of $\log(C_R/T)$ versus $1/T$ as depicted in Fig. 11 yielded straight lines from which the values of ΔH^* and ΔS^* were computed from the slope ($-\Delta H^*/2.303R$) and intercept [$\log(R/Nh) + (\Delta S^*/2.303R)$], respectively and listed in Table 5. The positive values of ΔH^* , both in the absence and presence of the inhibitor reflect the endothermic nature of the activated-complex formation from the reactants for the rate determining step of the steel dissolution process and this is considered in the literature as an indication of a hindered process of dissolution of steel (Zerga et al. 2010). Generally, when this process is exothermic, it is regarded as corresponding to either physisorption or chemisorption, while an endothermic formation of the intermediate reaction state is unequivocally attributed to chemisorptions Durnie et al. 1999). It can also be observed in Table 5 that E_a and ΔH^* vary in the same manner but the values of ΔH^* are lower than those of E_a . This has been reported (Ekanem et al. 2010; Noor 2007) as an indication that the corrosion process must involve a gaseous reaction, simply hydrogen evolution

reaction associated with a decrease in total reaction volume. The values of ΔS^* in the absence and presence of chitosan are negative (Table 5) which indicates that the activated complex in the rate-determining step represents an association rather than a dissociation process. Consequently, a decrease in disordering takes place on going from reactants to activated complex. Similar observations have been reported in the literature for mild steel dissolution in the absence and presence of inhibitors in HCl solution (Popova et al. 2003; Noor and Al-Moubaraki 2008). Also, ΔS^* values become more negative as the chitosan concentration increases, showing more ordered behaviour leading to an increase in inhibition efficiency.

PZC and corrosion inhibition mechanism

The efficiency of an organic compound as a successful inhibitor is mainly dependent on its ability to get adsorbed on the metal surface. Corrosion inhibition is initiated by the displacement of adsorbed water molecules by the inhibitor species leading to specific adsorption of the inhibitor on the metal surface as:



The process of adsorption is influenced by the nature and charge of the metal, by the chemical structure of the organic inhibitor and the type of aggressive electrolyte. The charge of the metal surface can be determined from the potential of zero charge (PZC) on the correlative scale (φ_c) by the equation (Hermas et al. 2004; Morad 2008):

$$\varphi_c = E_{\text{corr}} - E_{q=0} \quad (19)$$

where $E_{q=0}$ is the potential of zero charge. The surface charge can be defined by the sign and absolute value of φ_c . If the net charge is negative, the adsorption of cations is favored. On the other hand, the adsorption of anions is favored if the net charge is positive.

In order to gain an insight into the surface charge of the mild steel, double layer capacitance (C_{dl}) was determined from the electrode's impedance measured at a single high frequency (1 kHz) under the assumption that the faradaic contribution to the overall measured impedance is negligible. Accordingly, C_{dl} was evaluated at different electrode potentials E in order to obtain $C_{dl} - E$ plots. The dependence of C_{dl} on the applied potential of mild steel in the inhibited 0.1 M HCl solution containing 4.0 μM chitosan after

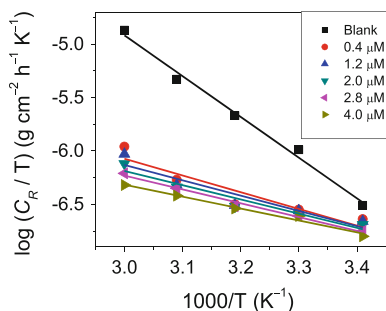


Fig. 11 Transition state plot for mild steel corrosion in 0.1 M HCl in the absence and presence of different concentrations of chitosan

1 h of immersion time is given in Fig. 12. The minimum of the curve at -615 mV (SCE), is ascribed to the PZC of the mild steel electrode in 0.1 M HCl solution containing $4.0 \mu\text{M}$ chitosan (Solmaz et al. 2008; Saleh 2006). E_{corr} of the mild steel in the same inhibited solution is -538 mV(SCE) resulting $\varphi_c = +78$ mV(SCE). This implies that the metal surface is positively charged at the corrosion potential after 1 h of exposure time.

From the obtained PZC values, it could be possible to propose a probable mechanism of corrosion inhibition of mild steel in 0.1 M HCl by chitosan. Chitosan molecules exist as protonated species in acidic solution in equilibrium with its corresponding neutral species, thus it is difficult for the protonated chitosan to approach the positively charged mild steel surface (H_3O^+ /metal interface) due to electrostatic repulsion. Therefore, Cl^- ions should be first adsorbed onto the positively charged metal surface due to a smaller degree of hydration, bringing excess negative charges close to the interface and favoring further adsorption of the positively charged inhibitor molecules. Thus, protonated chitosan molecules adsorb, through electrostatic interactions, on the negatively charged metal surface to form a protective layer. It is not possible to rule out that the protonated chitosan molecules may also be adsorbed on the negatively charged metal surface (cathodic sites) in competition with hydrogen ions to reduce the rate of hydrogen evolution reaction, as reported for a comparable system (Yüce and Kardas 2012). However, in addition to the physical adsorption, the cationic and neutral molecules become adsorbed on the positively charged metal surface (anodic sites) through the chemisorption mechanism, involving the displacement of water molecules from the mild steel surface and the

sharing of electrons between free electron pairs of heteroatoms and vacant d orbitals of iron. This is clearly manifested from the observed increase in inhibition efficiency with increase in temperature, which characterizes chemical adsorption phenomena. Noteworthy, the adsorption of chitosan is comprehensive, including predominantly chemical adsorption as also shown by the values of ΔG_{ads}^0 and kinetic considerations.

Some authors (Abdallah and El-Naggar 2012; Obot et al. 2011) claimed that corrosion inhibition effects on metals in the presence of an inhibitor may arise from a complex formation involving the metal and the inhibitor. In order to gain an insight into the possibility of the occurrence of a complexation reaction between mild steel and chitosan, UV–visible spectroscopic measurements were undertaken since it has been reported that a change in position of the absorbance maximum and a change in the value of absorbance indicate the formation of a complex between two species in solution (Abboud et al. 2007). Figure 13

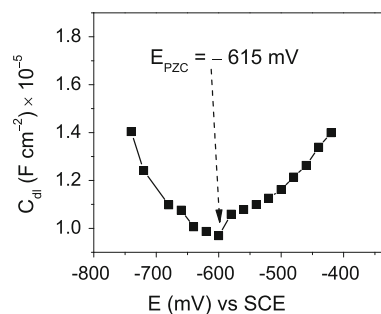


Fig. 12 Plot of C_{dl} against applied potential E for mild steel in 0.1 M HCl containing $4.0 \mu\text{M}$ chitosan

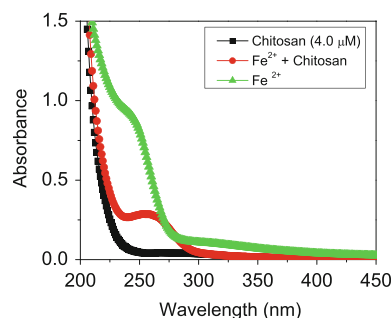


Fig. 13 UV-visible spectra of (dash with square) 0.1 M HCl with $4.0 \mu\text{M}$ chitosan added; (dash with circle) 0.1 M HCl with $4.0 \mu\text{M}$ chitosan added after mild steel immersion, 5 h at 70°C ; (dash with triangle) 0.1 M HCl after mild steel immersion, 5 h at 70°C

shows UV–visible absorption spectra measured for 0.1 M HCl solution without and with 4.0 μM chitosan before and after 5 h of mild steel immersion at 70 °C. The absorption spectrum of the solution resulting from mild steel immersion in 0.1 M HCl containing

chitosan is different from the other two spectra. This solution shows a low intensity band with an absorption maximum at ca. 263 nm, while the spectrum for chitosan in 0.1 M HCl shows no absorption band in this ultraviolet region. The solution resulting after 5 h immersion of mild steel in 0.1 M HCl without added chitosan displays a more intense absorption band (as a shoulder) at ca. 251 nm. After 5 h of immersion, formation of new products in the solution is evident. The differences observed between the three spectra in Fig. 13 are indicative of the characteristic pattern of complex formation between chitosan and metal ions released during the corrosion reaction. Owing to the presence of functional groups, chitosan is highly capable of metal coordination (Vlasov et al. 2009).

Surface morphological examination

The surface morphologies of unexposed mild steel and the ones exposed to 0.1 M HCl solution in the absence and presence of 0.4 μM chitosan after 5 h immersion at 40 °C were examined using SEM. The results shown in Fig. 14 reveal that the mild steel specimens had very rough surface in the absence of chitosan (Fig. 14b) as expected due to corrosive attack of the acid solution. The attack was relatively uniform with slight evidence of selective corrosion (compare Fig. 14b with Fig. 14a for unexposed mild steel). In the presence of chitosan (Fig. 14c) surface roughness is reduced indicating the inhibiting effect of chitosan on the surface.

Conclusions

Chitosan (a naturally occurring polymer) in unmodified form has been evaluated for its potential to reduce corrosion attack of mild steel in corrosive acidic environment. From the results obtained, the following conclusions can be drawn:

- (1) Chitosan acts as an efficient inhibitor for mild steel corrosion even at very low concentrations. Inhibition efficiency increases with increase in temperature.
- (2) Corrosion inhibition is afforded by virtue of adsorption of chitosan onto mild steel surface which is found to accord with Langmuir adsorption isotherm.

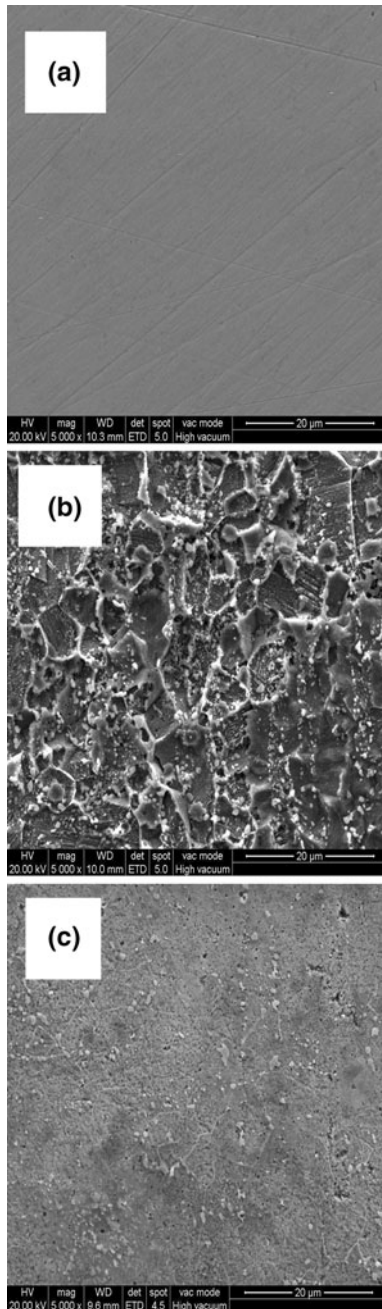


Fig. 14 SEM images for **a** unexposed mild steel; **b** exposed mild steel in blank solution, and **c** exposed mild steel in 0.1 M HCl containing 4.0 μM chitosan, at 40 °C for 5 h

- (3) The results of potentiodynamic polarization measurements point to chitosan functioning as a mixed inhibitor affecting both the anodic and cathodic reactions.
- (4) The phenomenon of chemical adsorption is proposed from the trend of increase in inhibition efficiency with increase in temperature which is corroborated by the values of kinetic and thermodynamic parameters obtained from the experimental data.

Acknowledgments S. A. Umoren acknowledges the Academy of Sciences for the Developing World (TWAS) for the TWAS-UNESCO Associateship appointment at INIFTA, CONICET Argentina and the Vice Chancellor, University of Uyo, Nigeria for granting Special Leave to visit INIFTA, Argentina, C.A. Gervasi gratefully acknowledges the Comisión de Investigaciones Científicas y Técnicas Buenos Aires (CICBA) for his position as a member of the Carrera del Investigador Científico. This work was partially financed with a grant from Agencia Nacional de Promoción Científica y Tecnológica (PICT N° 2008-1902), and M.V. Mirífico gratefully acknowledges the Consejo Nacional de Investigaciones Científicas y Técnicas (CONICET-CCT LP) (PIP 0847), Universidad Nacional de La Plata (UNLP), and Facultad de Ingeniería UNLP, Área Departamental de Ingeniería Química (11-I133).

References

- Abboud Y, Abourriche A, Saffaj T, Berrada M, Charrouf M, Bennamara A, Himidi N, Hannache H (2007) 2,3-Quinoxalinedione a novel corrosion inhibitor for mild steel in 1 M HCl. *Mater Chem Phys* 105:1–5
- Abd El Rehim SS, Hassan HH, Amin MA (2001) Corrosion inhibition of aluminum by 1,1(lauryl amido)propyl ammonium chloride in HCl solution. *Mater Chem Phys* 70:64–72
- Abdallah M (2004) Guar gum as corrosion inhibitor for carbon steel in sulphuric acid solutions. *Portug Electrochim Acta* 22:161–175
- Abdallah M, El-Naggar MM (2012) Cu^{2+} cation + 3,5-dimethylpyrazole mixture as a corrosion inhibitor for carbon steel in sulfuric acid solution. *Mater Chem Phys* 71:291–298
- Ahamad I, Prasad R, Quraishi MA (2010) Adsorption and inhibitive properties of some new Mannich bases of Isatin derivatives on corrosion of mild steel in acidic media. *Corros Sci* 52:1472–1481
- Amin MA, Ahmed MA, Arida HA, Arslan T, Saracoglu M, Kandemirli F (2011) Monitoring corrosion and corrosion control of iron in HCl by non-ionic surfactants of the TRITON-X series—part II. Temperature effect, activation energies and thermodynamics of adsorption. *Corros Sci* 53:540–548
- Atkins PW (1990) *Physical chemistry*, 4th edn. Oxford University Press, Oxford
- Bai L, Conway BE (1991) AC impedance of Faradaic reactions involving electroadsorbed intermediates: examination of conditions leading to pseudoinductive behavior represented in three-dimensional impedance spectroscopy diagrams. *J Electrochem Soc* 138:2897–2907
- Bayol E, Gurten AA, Dursun M, Kayakirilmaz K (2008) Adsorption behaviour and inhibition corrosion effect of sodium carboxymethyl cellulose on mild steel in acidic medium. *Acta Physico-Chim Sinica* 24:2236–2242
- Behpour M, Ghoreishi SM, Gandomi-Niasar A, Soltani N, Salavati-Niasari M (2009a) The inhibition of mild steel corrosion in hydrochloric acid media by two Schiff base compounds. *J Mater Sci* 44:2444–2453
- Behpour M, Ghoreishi SM, Khayatkashani M, Soltani N (2009b) The effect of two oleo-gum resin exudate from *Ferula assa-foetida* and *Dorema ammoniacum* on mild steel corrosion in acidic media. *Corros Sci* 53:2489–2501
- Boukamp BAA (1986) Nonlinear least squares fit procedure for analysis of impedance data of electrochemical systems. *Solid State Ionics* 20:31–44
- Buchweishajja J, Mhinzi GS (2008) Natural products as a source of environmentally friendly corrosion inhibitors: the case of gum exudate from *Acacia seyal* var. *seyal*. *Portug Electrochim Acta* 26:257–265
- Cao C (1996) On electrochemical techniques for interface inhibitor research. *Corros Sci* 38:2073–2082
- Cheng S, Chen S, Liu T, Chang X, Yin Y (2007) Carboxymethyl chitosan + Cu^{2+} mixture as an inhibitor used for mild steel in 1.0 M HCl. *Electrochim Acta* 52:5932–5938
- Durnie W, De Marco R, Jefferson A, Kinsella B (1999) Development of a structure-activity relationship for oil field corrosion inhibitors. *J Electrochem Soc* 146:1751–1756
- Ekanem UF, Umoren SA, Udousoro II, Udoh AP (2010) Inhibition of mild steel corrosion in HCl using pineapple leaves (*Ananas comosus* L.) extract. *J Mater Sci* 45:5558–5566
- El-Haddad MN (2013) Chitosan as a green inhibitor for copper corrosion in acidic medium. *Int J Biol Macromol* 55:142–149
- Fekry AM, Mohamed RR (2010) Acetyl thiourea chitosan as an eco-friendly inhibitor for mild steel in sulphuric acid medium. *Electrochim Acta* 55:1933–1939
- Ferreira EdeMM, Morelli T, Moreira IMNS, de Carvalho SMS (2004) Studies on indium sorption from iodide medium by polyurethane foam. *J Braz Chem Soc* 15:563–569
- Fu J, Zang H, Wang Y, Li S, Chen T, Liu X (2012) Experimental and theoretical study on the inhibition performances of quinoxaline and its derivatives for the corrosion of mild steel in hydrochloric acid. *Ind Eng Chem Res* 51:6377–6386
- Hermas AA, Morad MS, Wahdan MH (2004) Effect of PgTPhPBr on the electrochemical and corrosion behaviour of 304 stainless steel in H_2SO_4 solution. *J Appl Electrochem* 34:95–102
- Jayakumar R, Prabakaran M, Reis RL, Mano JF (2005) Graft copolymerized chitosan—present status and applications. *Carbohydr Polym* 62:142–158
- Jones DA (1992) Principles and prevention of corrosion. In: Johnstone D (ed). Macmillan Publishing Company, NY
- Khairou KS, El-sayed A (2003) Inhibition effect of some polymers on the corrosion of cadmium in hydrochloric acid solution. *J Appl Polym Sci* 88:866–871
- Khaled KF, Al-Qahtani MM (2009) The inhibitive effect of some tetrazole derivatives towards Al corrosion in acid solution: chemical, electrochemical and theoretical studies. *Mater Chem Phys* 113:150–158

- Khaled KF, Babić-Samardžija K, Hackerman N (2006) Cobalt(III) complexes of macrocyclic-bidentate type as a new group of corrosion inhibitors for iron in perchloric acid. *Corros Sci* 48:3014–3034
- Machnikova E, Whitmire KH, Hackerman N (2008) Corrosion inhibition of carbon steel in hydrochloric acid by furan derivatives. *Electrochim Acta* 53:6024–6032
- Mansfeld F (1973) Tafel slopes and corrosion rates from polarization resistance measurements. *Corrosion* 29:397–402
- Mansfeld F (1999) Analysis and Interpretation of EIS Data for Metals and Alloys, Technical Report N° 26, Part No.: BTR026. Issue: AB: May 1999, Solartron Ltd., LA
- Martinez S, Stern I (2001) Inhibitory mechanism of low-carbon steel corrosion by mimosa tannin in sulphuric acid solutions. *J Appl Electrochem* 31:973–978
- Metikos-Hukovic M, Babic R, Grubac Z (2002) The study of aluminium corrosion in acidic solution with nontoxic inhibitors. *J Appl Electrochem* 32:35–41
- Mobin M, Khan MA, Parveen M (2011) Inhibition of mild steel corrosion in acidic medium using starch and surfactants additives. *J Appl Polym Sci* 121:1558–1565
- Mohamed RR, Fekry AM (2011) Antimicrobial and anticorrosive activity of adsorbents based on chitosan Schiff's base. *Int J Electrochem Sci* 6:2488–2508
- Morad MS (2008) Inhibition of iron corrosion in acid solutions by Cefatrexyl: behaviour near and at the corrosion potential. *Corros Sci* 50:436–448
- Mortimer RG (2000) Physical chemistry, 2nd edn. Academic Press, San Diego
- Nataraja SE, Venkatesha TV, Manjunat K, Poojary B, Pavithra MK, Tandon HC (2011) Inhibition of the corrosion of steel in hydrochloric acid solution by some organic molecules containing the methylthiophenyl moiety. *Corros Sci* 53:2651–2659
- Noor EA (2007) Temperature effects on the corrosion inhibition of mild steel in acidic solutions by aqueous extract of Fenugreek leaves. *Int J Electrochem Sci* 2:996–1017
- Noor EA (2009) Evaluation of inhibitive action of some quaternary N-heterocyclic compounds on the corrosion of Al–Cu alloy in hydrochloric acid. *Mater Chem Phys* 114:533–541
- Noor EA, Al-Moubaraki AH (2008) Thermodynamic study of metal corrosion and inhibitor adsorption processes in mild steel/1-methyl-4[4'(-X)-styryl pyridinium iodides/hydrochloric acid systems. *Mater Chem Phys* 110:145–154
- Obi-Egbedi NO, Obot IB (2011) Inhibitive properties, thermodynamic and quantum chemical studies of alloxazine on mild steel corrosion in H₂SO₄. *Corros Sci* 53:263–275
- Obot IB, Obi-Egbedi NO, Eseola AO (2011) Anticorrosion potential of 2-Mesityl-1H-imidazo [4,5-f][1,10]-phenanthroline on mild steel in sulfuric acid solution: experimental and theoretical study. *Ind Eng Chem Res* 50:2098–2110
- Oguzie EE (2006) Studies on the inhibitive effect of *Occimum viridis* extract on the acid corrosion of mild steel. *Mater Chem Phys* 99:441–446
- Oguzie EE, Li Y, Wang FH (2007) Corrosion and corrosion inhibition characteristics of bulk nanocrystalline ingot iron in sulphuric acid. *J Solid State Electrochem* 12:721–728
- Okafor PC, Zheng Y (2009) Synergistic inhibition behaviour of methylbenzyl quaternary imidazoline derivative and iodide ions on mild steel in H₂SO₄ solutions. *Corros Sci* 51:850–859
- Popova A, Sokolova E, Raicheva S, Christov M (2003) AC and DC study of the temperature effect on mild steel corrosion in acid media in the presence of benzimidazole derivatives. *Corros Sci* 45:33–58
- Rinaudo M, Pavlov G, Desbrieres J (1999) Influence of acetic acid concentration on the solubilization of chitosan. *Polymer* 40:7029–7032
- Rosliza R, Wan Nik WB (2010) Improvement of corrosion resistance of AA6061 alloy by tapioca starch in seawater. *Curr Appl Phys* 10:221–229
- Saleh MM (2006) Inhibition of mild steel corrosion by hexadecylpyridinium bromide in 0.5 M H₂SO₄. *Mater Chem Phys* 98:83–89
- Singh AK (2012) Inhibition of mild steel corrosion in hydrochloric acid solution by 3-(4-((Z)-Indolin-3-ylideneamino)phenylimino) indolin-2-one. *Ind Eng Chem Res* 51:3215–3223
- Solmaz R, Kardas G, Yazici B, Erbil M (2008) Adsorption and corrosion inhibitive properties of 2-amino-5-mercapto-1,3,4-thiadiazole on mild steel in hydrochloric acid media. *Coll Surf A Physicochem Eng Aspects* 312:7–17
- Solomon MM, Umoren SA, Udoso II, Udoh AP (2010) Inhibitive and adsorption behaviour of carboxymethyl cellulose on mild steel corrosion in sulphuric acid solution. *Corros Sci* 52:1317–1325
- Stupnišek-Lisac E, Gazivoda A, Madžarac M (2002) Evaluation of non-toxic corrosion inhibitors for copper in sulphuric acid. *Electrochim Acta* 47:4189–4194
- Umoren SA (2008) Inhibition of aluminium and mild steel corrosion in acidic medium using gum Arabic. *Cellulose* 15:751–761
- Umoren SA (2011) Synergistic inhibition effect of polyethylene glycol—polyvinyl pyrrolidone blends for mild steel corrosion in sulphuric acid medium. *J Appl Polym Sci* 119:2072–2084
- Umoren SA, Obot IB, Ebenso EE, Okafor PC, Ogbo O, Oguzie EE (2006) Gum arabic as a potential corrosion inhibitor for aluminium in alkaline medium and its adsorption characteristics. *Anti Corros Methods Mater* 53:277–282
- Umoren SA, Obot IB, Ebenso EE, Okafor PC (2008) Eco-friendly inhibitors from naturally occurring exudates gums for aluminium corrosion inhibition in acidic medium. *Portug Electrochem Acta* 26:267–282
- Umoren SA, Obot IB, Obi-Egbedi NO (2009) *Raphia hookeri* gum as a potential eco-friendly inhibitor for mild steel in sulphuric acid. *J Mater Sci* 44:274–279
- Villamil RFV, Corio P, Rubín JC, Agostinho SML (1999) Effect of sodium dodecylsulfate on copper corrosion in sulfuric acid media in the absence and presence of benzotriazole. *J Electroanal Chem* 472:112–119
- Vlasov PS, Kiselev AA, Domnina NS, Popova EV, Tyuterev SL (2009) Synthesis and biological activity of metal chitosan complexes. *Russ J Appl Chem* 82:1675–1681
- Yang KK, Wang XL, Wang YZ (2007) Progress in nanocomposite of biodegradable polymer. *J Ind Eng Chem* 13:485–500

- Yüce AO, Kardas G (2012) Adsorption and inhibition effect of 2-thiohydantoin on mild steel corrosion in 0.1 M HCl. *Corros Sci* 58:86–94
- Zarrouk A, Hammouti B, Zarrok H, Al-Deyab SS, Messali M (2011) Temperature effect, activation energies and thermodynamic adsorption studies of L-cysteine methyl ester hydrochloride as copper corrosion inhibitor in nitric acid 2 M. *Int J Electrochem Sci* 6:6261–6274
- Zerga B, Attayibat A, Sfaira M, Taleb M, Hammouti B, Ebn Touhami M, Radi S, Rais Z (2010) Effect of some tripodal bipyrazolic compounds on C38 steel corrosion in hydrochloric acid solution. *J Appl Electrochem* 40:1575–1582